International Journal of Control and Automation
Vol. 7, No. 12 (2014), pp. 375-382
http://dx.doi.org/10.14257/ijca.2014.7.12.34

Research on Preparation of Ni/SiO_2 Optical Attenuation Slice by Magnetron Sputtering

Lei Li, Hui Tang, Shanshan Hao and Wenxue Wang

School of Materials Science and Engineering Harbin University of Science and Technology CHINA 150040
tanghui6003@sina.com

Abstract

In order to find new methods for preparing and improving the performance of optical attenuation slice. Vacuum magnetron sputtering method was used to prepare Ni/SiO_2 composite film optical attenuation slices, with vacuum magnetron sputtering apparatus, at 5,10,15,20,25min sputtering time, 0.2,0.4,0.6,0.8,1.0Pa sputtering pressure and sputtering power 300~1200W. The XRD, SEM, EDS, AFM and 722 spectrophotometer also were used to study the effects of different sputtering time, sputtering pressure and sputtering power on the film structure, surface morphology, composition, three-dimensional structure, surface roughness and light attenuation rate of optical attenuation slice samples. The results indicated that: Ni/SiO2 composite films were formed, instead of simple physical adsorption between Ni film and SiO2 substrates with magnetron sputtering by XRD analysis and calculation, with uniform grain size of 25.96, 32.38, 32.29,26.95, 25.92nm, respectively. The main component element was Ni, but there were few impurities deposited on the substrates. Impurities were reduced gradually with the increase of sputtering time, mainly resulted from two sputtering of Ni atoms by EDS; The film surface was smooth and dense, flatness and organizational structure of Ni film were better, surface roughness was 1.267nm at 25min sputtering time, 0.4Pa pressure and 400W power with SEM and AFM. Light attenuation rate of optical attenuation slices was different in different process parameters, and the maximum reached 0.52, film flatness, impurities and defects were the main reason by the light attenuation performance analysis.

Keywords: *optical attenuation slice, magnetron sputtering, attenuation ratio*

1. Introduction

Because of the uncertainty of signal source and transmission distance in optical fiber communication, the signal intensity in the line may be too large, resulting in many negative phenomenons, such as distortion of optical signal transmission, error of images and data transmission in communication system [1]. Therefore, power was required not to exceed the critical value in the actual communication process. To meet the technical requirements, measures should be taken to control the optical power [2]. Optical attenuator is a kind of optical devices, which could reduce and control the light signal, equalize received power of the channel and decline bit error probability, etc. Optical attenuation slice is the key component of optical attenuator [3]. Currently, many kinds of methods are used to prepare optical attenuation slice, including electroplating, chemical plating, vacuum evaporation plating *etc.,* but these methods pollute environment, and more importantly, their uncontrolledly thick film [4-5]. So searching for a new method for the preparation of optical attenuation slice becomes the key to solve problems. Magnetron sputtering [6-8] is one of the most promising surfaces coating technology because of its advanced process, high deposition

ISSN: 2005-4297 IJCA
Copyright ⓒ 2014 SERSC

rate, low substrate temperature, good film adhesion and no pollution [9-12]. Based on this, metal Ni /SiO_2 composite film optical attenuation slice samples were prepared, plating Ni on SiO_2 glass substrates by magnetron sputtering technology. The surface morphology, crystal structure, three-dimensional structure, roughness and attenuation ratio of process variables on the metal Ni /SiO2 composite thin film optical attenuation slice samples were studied.

2. Experimental

Firstly, glass substrates were treated for degreasing and cleaning in ultrasound, cleaned in acetone solution of 30min, then washed with ethanol 10min, and then cleaned with deionized water, dried spare. The metal Ni target was fixed on the electromagnetic target location, SiO_2 glass substrates were put into the specimen shelf. According to the experiment requirement to adjust the temperature, temperature was 25℃. The molecular pump, power taps and mechanical pump were started to pump base vacuum. In order to reduce the residual gas in the vacuum cavity and ensure the purity of the film, molecular pump was opened to pump high vacuum when pressure was less than 10Pa. Pure Ar (99.999%) was passed when vacuum degree reached 5×10^{-3}Pa. Pure Ar as the working gas, the oxide layer and pollutants of the target surface were removed with pre sputtering of 10min and ion etching of 20min before deposition of Ni film. Sputtering power was opened to sputter, Ar+ ions were formed from Ar gas in high voltage current. Ni target was bombarded by Ar+, Ni atoms escaped and were deposited on the surface of the SiO_2 substrate, Ni film was formed. All power source were closed after reaction, cooling and sampling. High-energy particle energy was converted into heat energy in sputtering process although low temperature, resulting in high substrate temperature, therefore samples could not be immediately removed.

3. Results and Discussion

3.1 Effect of Sputtering Pressure on the Film Structure

Figure 3-1 represented XRD patterns of films with different sputtering pressure.

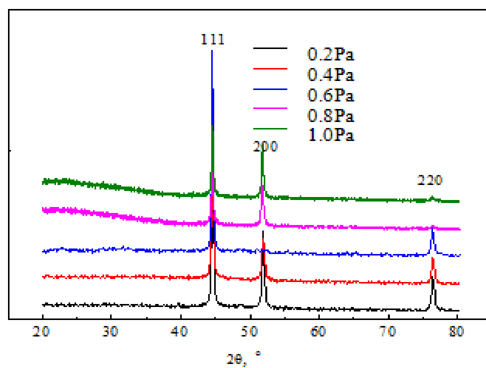

Figure 3-1. XRD Patterns of Films with Different Sputtering Pressure

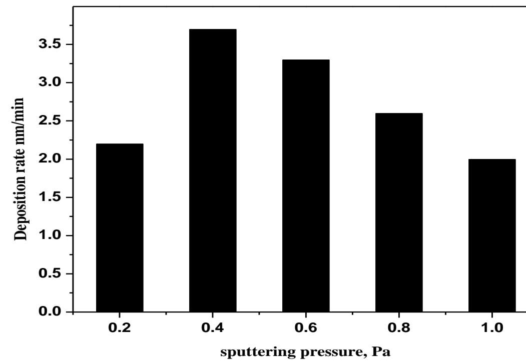

Figure 3-2. Deposition Rate with Different Sputtering Pressure

The diffraction peaks of Ni films were consistent with standard card(JCPDS6-585) diffraction peaks of metal Ni, which certified the coating layers were pure nickel film, in which all the peak intensity of specimens in the (111) diffraction peak direction were maximum. It suggested that, Ni film grew with preferred orientation on the Ni(111). With the increasing of sputtering pressure, diffraction peak intensity of nickel film on the (111)

 Copyright ⓒ 2014 SERSC

increased first and then decreased. With a maximum of 0.6Pa, intensity of (111) at 0.8Pa decreased, but intensity of Ni (200) significantly enhanced. With the growth of Ni atom in (111), when Ni atoms were so excessive, leading to too large steric hindrance. In contrast, less steric hindrance and smaller particle scattering of Ni (200), were more conducive to the preferential growth of Ni film [13].

The deposition rate of films with different deposition pressure was shown in Figure 3-2. The deposition rate was relatively low at sputtering pressure of 0.2pa, with increasing of sputtering pressure, the deposition rate increased, and reached a maximum value at sputtering pressure of 0.4Pa, then declined. Because of larger mean free path of charged particles at lower sputtering pressure, sputtered nickel atoms with greater kinetic energy were easily deposited on the substrate surface. But fewer high-energy Ar+ bombarding Ni target in reaction chamber resulted in lower sputtering rate and deposition rate relatively. Sputtering rate was increased with increased Ar+, which was not enough to influence the mean free path of particles when sputtering pressure was higher. But when argon content was increased to a certain value, gas density in the reaction chamber increased, so that the chances of collisions between high-energy particles bombarding Ni target and argon molecules or high energy particles and high energy particles were increased. Consequently, the mean free path and average kinetic energy of sputtered nickel atoms also were reduced, partial sputtered atoms could not reach substrate surface, which causing lower sputtering rate. Declining of average kinetic energy made migration of sputtered atoms in the membrane surface decrease, aggregation of atoms made more rough film surface and more grain gap at a high working pressure [14].

Scherer equation [15] was used to calculated grain size according to half high width and Cape Prague from Figure 3-1 at different pressures, as shown in Table 3-1.

Table 3-1. Particle Size of Ni Coating with Different Sputtering Pressure

Pressure, Pa	Half high width, Rad	Cape Prague,°	particle size , nm
0.2	0.00571	22.26826	25.96
0.4	0.00458	22.30099	32.38
0.6	0.00474	22.30099	32.29
0.8	0.00550	22.25123	26.95
1.0	0.00572	22.29718	25.92

Particle sizes were first increased and then decreased with the increasing of sputtering pressure. Higher sputtering rate and larger surface migration amount of nickel atoms leading to greater opportunities of direct collisions nucleation among Ni atoms and larger grain size.

3.2 Effect of Sputtering Time on the Film Surface Morphology

Surface of optical attenuation slice layer was required smooth when transmission of optical signal, otherwise uneven film thickness would lead to the different light attenuation and signal distortion. Therefore surface morphology of nickel film needed to be studied. To know the effect of sputtering time in magnetron sputtering process, surface morphology of metal Ni films were tested. Figure 3-3 showed SEM images of Ni film in different sputtering time (a,b,c,d and e represented SEM images of 5,10,15,20 and 25min sputtering time, respectively).

Copyright ⓒ 2014 SERSC

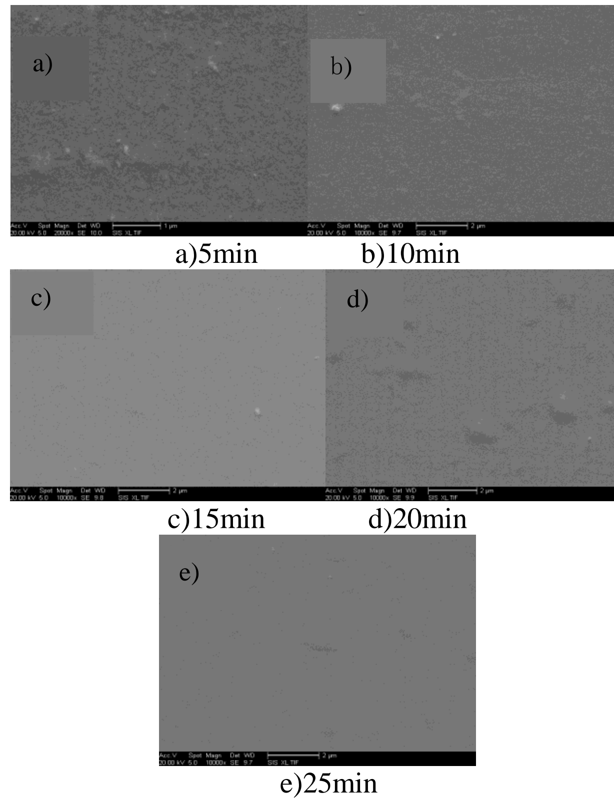

Figure 3-3. SEM Images of Ni Film in Different Sputtering Time

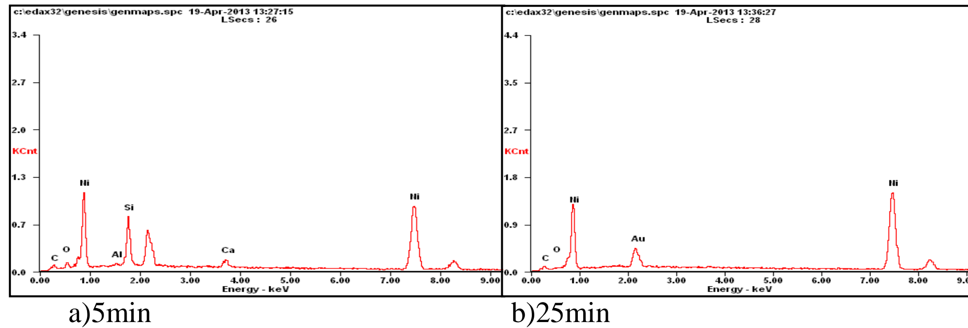

Figure 3-4. EDS Patterns with Different Sputtering Time

The surface of sample a was dense but not flat, many small convexities were adhered on coating surface; With the sputtering time increasing, less small convexities and more and more smooth films were distributed on surface. Particles on the film surface were distributed evenly and compactly, almost no convex mounds and other defects at 25min in Figure 3-4 showed EDS patterns with different sputtering time.

In summary, EDS and SEM images analysis showed that, convex mounds in Ni films, were caused by reunion of nickel atoms. When sputtering time was short, sputtered nickel atoms had no time to nucleated, particles were tiled in a simple manner on a substrate. But magnetron sputtering was an irregular movement, nickel atoms were prone to non-uniform or to be reunited grown on the substrate. Since the target contained a small amount of impurities, nickel atoms and impurities were sputtered onto the substrate together. In Figure 3-4, film

 Copyright ⓒ 2014 SERSC

contained impurities Al at 5min, but at 25min, film did not. Because of short sputtering time, impurities and nickel atoms were bombard out by sputtering on substrate, and embedded in film. As time increased, the sputtered nickel atoms also played the role of correction. In other word, nickel atoms bombarded the growing film, controlled and changed the structure and properties of thin film by the action of bombardment or embedded. Thus, impurities and aggregative nickel atoms secondary sputtered, impurities were separated from films, aggregative atoms were dispersed and re-deposited on the substrates due to impact of Ar+.

3.3 Effect of Sputtering Power on Micro Structure and Flatness

To study the effect of sputtering power on the surface morphology of the film in process of magnetron sputtering, similar to other process conditions in the experiments, the work pressure and sputtering time were 0.4 Pa and 10 min, respectively, surface morphologies of metal Ni film were tested under different sputtering powers. SEM image of Ni membrane at 300 W was shown in Figure 3-5.

Ni film was very thin though Ar^+ could glow discharged normally, and even a complete coating had not yet be formed in some areas at 300W. The sputtering power was too small in the process of sputtering, the sputtering power was not completely used for sputtering, but for fever of target materials, X-ray emission, secondary electron emission and so on. The several kinds of posterior energy consumption could be thought of useless. Therefore, when the sputtering power was small, useful work could not meet the requirements, which led to weak bond of membrane layer and base. Glow discharge and sputtering were unable to proceed when the power was lower. So the sputtering power should be increased appropriately. SEM micrographs were shown in Figure 3-6.

Increasing the sputtering power to 400 W or 600 W, the membrane surface was smooth and compact with uniform particle distribution, small convex dome was hardly seen in figure 3-5 a) and b); Continuing to increase the sputtering power to 1000 W or 2000 W, white convex dome and groove could be seen clearly in the membrane surface and the roughness of the surface was poor in Figure 3-5 c) and d).

Because of bombarding particles with smaller energy, surface diffusion of sediment particles played a leading role in the range of sputtering power. Filling cavities of the surface constantly led to smooth surface. When the sputtering power was beyond this range, temperature of the target material was increased as a result of too high sputtering yield. The target surface corrosion caused low utilization rate of target material. Increasing condensation nuclei of sputtering atoms in the substrate was caused by large sputtering power. While the energy of condensation nuclei was increased, larger stress was existed within membrane layer, which led to low adhesive force and uneven surface. Sputtering power was large to cause the phenomenon of ion implantation and lower deposition rate. Therefore, choosing appropriate sputtering power had an important influence on smoothness, compactness and uniform light attenuation of membrane layer.

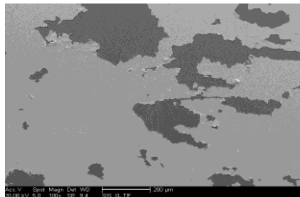

Figure 3-5. SEM Image of Ni Membrane at 300 W

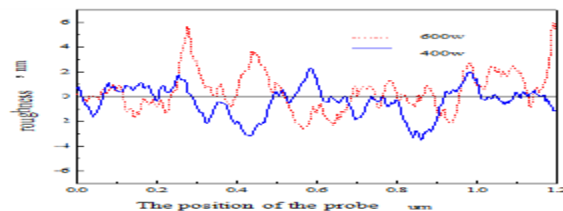

Figure 3-9. Surface Roughness of Ni Coating

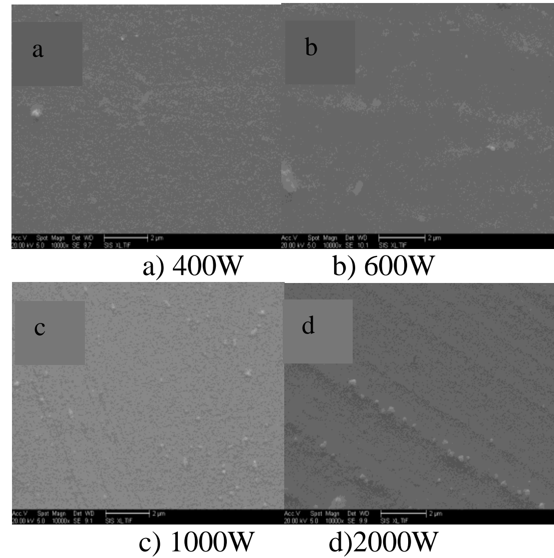

a) 400W b) 600W

c) 1000W d)2000W

Figure 3-6. SEM Images of Ni Film with Different Sputtering Power

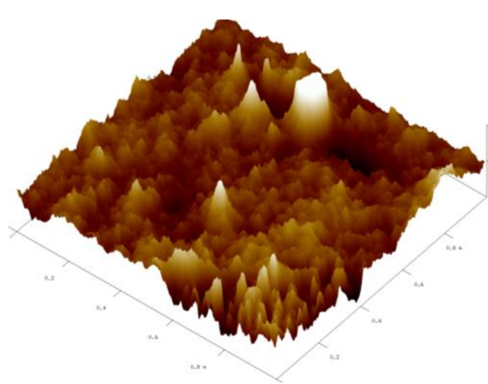

Figure 3-7. Three-dimensional Diagram with Sputtering Power of 400W

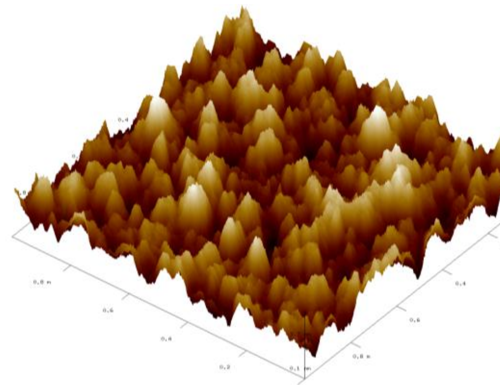

Figure 3-8. Three-dimensional diagram with Sputtering Power of 600W

AFM was used to further analyze roughness of film surface, Figure 3-7 and Figure 3-8 illustrated three-dimensional structures in different sputtering power, respectively. Relative roughness of film surface was shown in Figure 3-9.

Nickel film surface profile waviness could be seen directly, curves showed further testing of film surface roughness. Results declared that, surface roughness of Ni film Ra value in scanning area is 1.267nm at 400W, while 2.316nm at 600W. All results showed smaller roughness and dense and more uniform distribution of particles at 400W. On the contrary, roughness and convex of film were increased, but was still relatively compact at 600W. Glow discharge produced more Ar+, the collision frequency of nickel atoms and Ar+ were increased, the diffusion kinetic energy of nickel atoms in film surface was reduced at 600W, so that grain crystal was larger, roughness was increased. This caused above [16].

 Copyright ⓒ 2014 SERSC

3.4 Effect of Sputtering Power on Transmittance

722 spectrophotometer was used to show transmittance at wavelength of 800nm. Corresponding optical attenuation rate was calculated, and analysis diagram of light attenuation change with the sputtering power was drew, as shown in Figure 3-10.

Attenuation rate of Ni/SiO2 optical attenuation slice was increased first and then decreased at 0.4Pa and 0.6Pa, it was not the ideal state that too large or too small sputtering power. Maximum light attenuation rate and excellent performance were reached at 600W, but poor surface morphology and flatness, not uniform power through optical attenuation slice at these conditions. Compared with 600W, organizational structure and surface morphology of Ni film were perfect, and little difference of light attenuation rate at 400W.

Figure 3-11 showed corresponding optical attenuation rate with the sputtering pressure. Light attenuation rate of Ni/SiO_2 optical attenuation slice samples increased first and then decreased with increasing of sputtering pressure in same sputtering power. Light attenuation rate reached maximum value at 0.4Pa. From the analysis of front, deposition rate of Ni film was the fastest at 0.4Pa, the film thickness and absorption degree of light reached maximum at the same time, so resulting in higher attenuation rate, also smooth surface and excellent organizational structure. Not high nickel film purity, thin film, rough surface and other causes led to lower absorption capacity of film to light at high pressure.

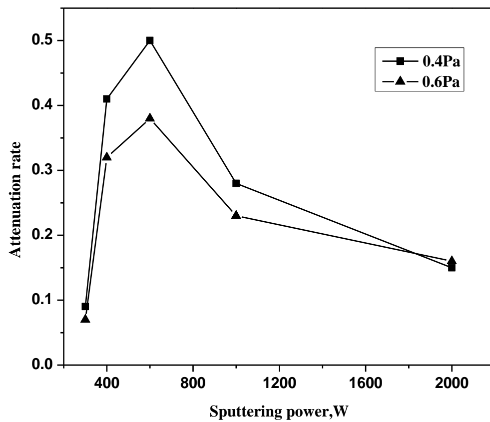

Figure 3-10. Attenuation Rate of Ni film with Different Sputtering Power

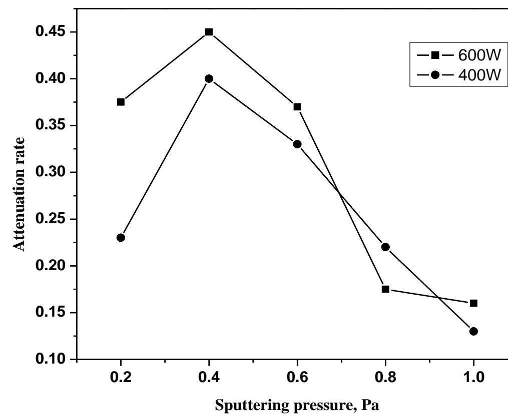

Figure 3-11. Attenuation rate of Ni Film with Different Sputtering Pressure

4. Conclusion

1) Ni/SiO2 composite films were formed, instead of simple physical adsorption between Ni film and SiO2 substrate with magnetron sputtering by XRD analysis and calculation, with uniform grain size of 25.96, 32.38, 32.29, 26.95, 25.92nm, respectively.

2) The main component element was Ni, but there were few impurities deposited on the substrates. Impurities were reduced gradually with the increase of sputtering time, mainly resulted from two sputtering of Ni atoms by EDS.

3) The film surface was smooth and dense, flatness and organizational structure of Ni film were better, surface roughness was 1.267nm at 25min sputtering time, 0.4Pa pressure and 400W power with SEM and AFM.

4) Light attenuation rate of optical attenuation slices was different in different process parameters, and the maximum reached 0.52, film flatness, impurities and defects were the main reason from the light attenuation performance analysis.

Copyright ⓒ 2014 SERSC

Acknowledgements

This work was supported in part by NSF Heilongjiang Province of China under Grant Nos.E201130.

References

[1] N. Takachio, H. Suzuki and Ishida, "WDM Linear Repeater Gain Scheme by Automatic Power Channel Selection for Photonic Transport Network", Optical Fiber Communication Conference and Exhibit, **(2004)**.
[2] Z. Y. Huang, "Optical Fiber Communication with New Optical Passive Device", Beijing University of Posts and Telecommunications Press, **(2003)**.
[3] S. L. Yang, "The Characteristics and Classification of China's Modern Optical Fiber Communication Technology", Public Communication of Science & Technology, **(2012)**, pp. 174-175.
[4] S. X. Chen, Z. F. Jiang and Y. F. Hu, "A Novel Method of Fabricating Graded Attenuating Thin Film Used for Variable Optical", Optical Communication Technology, vol. 29, no. 4, **(2005)**, pp. 4.
[5] L. Han, "Properties of Nickel Coating Deposited on Glass by DC Magnetron Sputtering", Surface Technology, vol. 41, no. 6, **(2012)**, pp. 65-69.
[6] J. F. Zhang, "Research on Preparation of Metal/SiO_2 Optical Attenuation Slice in Green Coating Technology", Harbin University of Science and Technology, **(2011)**, pp. 1-41.
[7] A. S. Reddya, H. H. Parka and S. Reddy, "Effect of sputtering power on the physical properties of DC magnetron sputtered copper oxide thin films", Materials Chemistry and Physics, vol. 110, **(2008)**, pp. 397-410.
[8] W. H. MA, Y. J. Zhai and C. L. Cai, "Study on Processing of Ni Thermo Sensitive Film by Magnetron Sputtering", Journal of Xi'An Technological University, no. 5, **(2011)**, pp. 409-412.
[9] M. Mccann, D. Mooney and M. Rahman, "Novel Nanoporous Silica and Titania Layers Fabricated by Magnetron Sputtering", ACS Applied Materials &Interfaces, vol. 3, no. 2 , **(2011)**, pp. 252-260.
[10] C. Becker and J. Petersen, "High Super Hydrophobicity on Poly (ethylene terephthalate) by Innovative Laser-Assisted Magnetron Sputtering", Journal of American Chemical Society, vol. 115, no. 4, **(2011)**, pp. 10675-10681.
[11] Y. L. Yang, J. W. Zhou, and Y. L. Liu, "Study on Amorphous Silicon Thin Films Deposited by DC Reactive Magnetron Sputtering", Electronic Design Engineering, vol. 18, no.4, **(2010)**, pp. 105-107.
[12] J. Q. Xu and L. X. Hang, "The Study of Magnetron Sputtering Ion Beam Density", Journal of Vacuum Science and Technology, vol. 24, no. 1, **(2011)**, pp. 74-76.
[13] T. Nishiyama, M. Ohtake, and F. Kirino, "Effects of Fcc Noble Metal Underlayer and Substrate Temperature on the Formation of Ni(111) Epitaxial Thin Films", IEEE, vol. 46, no. 6, **(2010)**, pp. 1491-1494.
[14] L. F. Yin, S. C. Wang and C. R. Zhang, "Effects of Preparation Technique on Deposition Rate of Silicon Nitride Coating by Low Pressure Chemical Vapor Deposition", Materials Review, no. S1, **(2008)**, pp. 443-445.
[15] X. C. Wang and X. Y. Zhang, "Modern Materials Analysis and Testing Technology", National Defence Industry Press, **(2009)**.
[16] B. Y. Jiang, J. Jiang and T. Feng, "Low energy Ar+ ion beam assisted deposition of Pt (111) preferred orientation films", Journal of functional materials, no. 6, **(2004)**.

Copyright ⓒ 2014 SERSC